Relative velocities in bidisperse turbulent aerosols: Simulations and theory

Akshay Bhatnagar,[1,*] K. Gustavsson,[2] B. Mehlig,[2] and Dhrubaditya Mitra[1,†]
[1]*Nordita, KTH Royal Institute of Technology and Stockholm University, Roslagstullsbacken 23, 10691 Stockholm, Sweden*
[2]*Department of Physics, Gothenburg University, 41296 Gothenburg, Sweden*

(Received 14 September 2018; published 13 December 2018)

We perform direct numerical simulations of a bidisperse suspension of heavy spherical particles in forced, homogeneous, and isotropic three-dimensional turbulence. We compute the joint distribution of relative particle distances and longitudinal relative velocities between particles of different inertia. For a pair of particles with small difference in their inertias we compare our results with recent theoretical predictions [Meibohm *et al.*, Phys. Rev. E **96**, 061102 (2017)] for the shape of this distribution. We also compute the moments of relative velocities as a function of particle separation and compare with the theoretical predictions. We observe good agreement. For a pair of particles that are very different from each other—one is heavy and the other one has negligible inertia—we give a theory to calculate their root-mean-square relative velocity. This theory also agrees well with the results of our simulations.

DOI: 10.1103/PhysRevE.98.063107

I. INTRODUCTION

Here we are concerned with small but heavy particles moving in a turbulent flow. How frequently and at what speeds do such particles collide with each other in turbulence? This question plays a central role in attempting to understand collisions and coalescence of microscopic water droplets in turbulent clouds [1] and to understand the formation of planetesimals in protoplanetary disks [2–4]. The particles in these turbulent aerosols are small and collisions between them are few and far between, consequently fluctuations matter. To understand how the distribution of particle sizes changes as a function of time, it is therefore not sufficient to merely consider the average collision rate. To account for the fluctuations it is necessary to consider the joint distribution of particle separations and their relative velocities [5–7]. A mean-field-like description based solely on the first moment of relative particle velocities neglects fluctuations and may therefore not be reliable.

Völk *et al.* [8–10] and others [11,12] formulated *inertial-range* theories for relative velocities of particles, referring to particle separations in the inertial range of turbulence. A criticism of this approach is that the collisions between the particles happen deep inside the dissipation range when the particle sizes are much smaller than the Kolmogorov length, η. It has been observed in direct numerical simulations (DNSs) that inertial-range theories for the moments of relative velocities [8–10] fail at small Stokes numbers [13] (the Stokes number is a dimensionless measure of the importance of particle inertia). The predictions of Ref. [12] for the far tail of the distribution of relative velocities between nearby identical particles assume large Stokes numbers and a well-developed inertial range. This is difficult to achieve in DNSs, and therefore it remains to be determined under which circumstances the prediction may hold.

Gustavsson *et al.* [6,14–16] developed a *dissipation-range* theory for the distribution of relative velocities of identical particles, when the collision radius—the sum of the particle radii—is in the dissipation range of turbulence. An asymptotic form of the distribution was obtained by matching two limiting cases and using that inertial particles of identical sizes distribute on a fractal attractor in phase space [6,14]. The result is a non-Gaussian distribution, with power-law tails that reflect large fluctuations. The theory applies in the limit where the Stokes number is large enough for particles to detach from the streamlines of the flow. But since the theory [6,14–16] neglects inertial-range fluctuations, it may require modifications at very large Stokes numbers where the particle separations explore the inertial range.

In the astrophysical literature, DNS results for the relative-velocity distribution were recently reported by Ishihara *et al.* [13], as well as by Pan and Padoan [17,18]. These authors fit the distribution to stretched exponentials. This raises the question how universal the power-law tails predicted in Refs. [6,14] are. For Stokes numbers of order unity, the power laws were clearly seen in DNSs [19,20].

The findings and open questions described above apply to identical particles. But to understand how the size distribution of particles in turbulent aerosols changes as a result of collisions and coalescences, the distribution for particles of different sizes (different Stokes numbers) is needed. Meibohm *et al.* [21] developed a *dissipation-range* theory for the distribution of relative velocities of particles that have different Stokes numbers, by analyzing a statistical model in the white-noise limit. The predictions of Ref. [21] have not been tested in DNSs yet.

To understand the distribution of relative velocities in turbulent aerosols is an important problem to study—both in theory and in simulations—because it is hard to obtain direct measurements of droplet velocities in clouds, and quite impossible as far as grain velocities in protoplanetary disks are concerned. There are two laboratory experiments [22,23]

*akshayphy@gmail.com
†dhruba.mitra@gmail.com

that have measured the distribution of relative velocities of micron-sized particles in turbulence and their mean and root-mean square values as functions of particle separations. Experimental limitations make it difficult to measure at which relative velocities particles actually collide in these experiments. For micron-sized particles this occurs at separations deep inside the dissipative range, at present outside the spatial resolution of the experiments.

It is therefore important to validate existing theories for collision velocities of particles in turbulence by comparison with results of DNSs. This is the purpose of the present paper. It is organized as follows: in Sec. II we describe the model and details of the DNSs. In Sec. III we summarize the key theoretical results of Refs. [14,21]. In Sec. IV we present our DNS results for the relative velocities between particles with different Stokes numbers. We compare the DNS results for the joint probability distribution of relative velocities and separations with the theoretical predictions of Meibohm *et al.* [21]. The distribution is non-Gaussian. When the difference between the Stokes numbers is not too large, then the distribution exhibits power-law tails as predicted by theory. At small separations and relative velocities, the power law in relative velocities is cut off, and it becomes a broad Gaussian (approximately uniform), verifying the new velocity scale V_c predicted by theory [21]. Also the distribution of separations becomes uniform for separations smaller than R_c. This scale was predicted in Refs. [24,25]. We show how the scales V_c and R_c are related. Finally, we develop a distinctive theory for the root-mean-square (RMS) relative velocities of particles when one of the particles has very small Stokes number. We find that the results from this theory are in accord with our simulations. We conclude in Sec. VI.

II. NUMERICAL METHOD

A. Particle dynamics

We describe the motion of a heavy particle in a turbulent flow by the Stokes model [26]:

$$\frac{d}{dt}\boldsymbol{x} = \boldsymbol{v}, \quad \frac{d}{dt}\boldsymbol{v} = \frac{1}{\tau}[\boldsymbol{u}(\boldsymbol{x},t) - \boldsymbol{v}]. \tag{1}$$

Here $\boldsymbol{x}$ and $\boldsymbol{v}$ are the position and velocity of the particle, respectively, and the characteristic response time of the particle is τ. The response time depends upon the particle size, a. In the Stokes limit, $\tau = (2\rho_p/9\rho)\,a^2/\nu$. Here ρ_p and ρ are the mass densities of the particle and the fluid, respectively, and ν is the kinematic viscosity. Finally $\boldsymbol{u}(\boldsymbol{x},t)$ is the flow velocity. This model assumes that the effect of gravitational acceleration is small compared to the acceleration due to the turbulent flow, fluid-inertia corrections are small, and both particle-particle interactions and Brownian diffusion of individual particles are ignored.

B. Direct numerical simulation of turbulence

The flow velocity $\boldsymbol{u}(\boldsymbol{x},t)$ is determined by solving the Navier-Stokes equation

$$\tfrac{\partial}{\partial t}\rho + \boldsymbol{\nabla}\cdot(\rho\boldsymbol{u}) = 0, \tag{2a}$$

$$\rho\tfrac{D}{Dt}\boldsymbol{u} = -\boldsymbol{\nabla}p + \mu\boldsymbol{\nabla}\cdot\mathbb{S} + \boldsymbol{f}. \tag{2b}$$

Here $\frac{D}{Dt} \equiv \partial_t + \boldsymbol{u}\cdot\boldsymbol{\nabla}$ is the Lagrangian derivative, p is the pressure of the fluid, and ρ is its density as mentioned above. The dynamic viscosity is denoted by $\mu \equiv \rho\nu$, and $\mathbb{S}$ is the second-rank tensor with components $S_{kj} \equiv \partial_k u_j + \partial_j u_k - \delta_{jk}(2/3)\partial_l u_l$ (Einstein summation convention). Here $\partial_k u_j$ are the elements of the matrix $\mathbb{A}$ of fluid-velocity gradients. We use the ideal gas equation of state with a constant speed of sound.

Our simulations are performed in a three-dimensional periodic box with sides $L_x = L_y = L_z = 2\pi$ in code units. To solve Eqs. (2) we use the pencil code [27], which uses a sixth-order finite-difference scheme for space derivatives and a third-order Williamson-Runge-Kutta [28] scheme for time derivatives. The external force $\boldsymbol{f}$, which is a white-in-time, Gaussian, stochastic process concentrated on a shell of wave number with radius k_f in Fourier space [29], is integrated by using the Euler-Marayuma scheme [30]. Under the action of the force the flow attains a statistically stationary state where the average energy dissipation by viscous forces is balanced by the average energy injection by the external force, $\boldsymbol{f}$. The amplitude of the external force is chosen such that the Mach number, $\mathrm{Ma} \equiv u_{\mathrm{rms}}/c_s$ (where c_s is the sound speed) is always less than 0.1, i.e., the flow is weakly compressible, which has no important effect on our results; please see the discussion in Ref. [20], Sec. II, and Appendix A there for further details. The same setup has been used in studies of scaling and intermittency in fluid and magnetohydrodynamic turbulence [31–33].

We introduce the particles into the simulation after the flow has reached a statistically stationary state. Initially, the positions of the heavy particles are random and statistically homogeneous with zero initial velocity. Then we simultaneously solve Eqs. (1) and (2). To this end we must interpolate the flow velocity to typically off-grid positions of the heavy inertial particles. We use a trilinear method for interpolation.

We define the Reynolds number by $\mathrm{Re} \equiv u_{\mathrm{rms}}/(\nu k_f)$, where u_{rms} is the root-mean-square velocity of the flow averaged over the whole domain and the kinematic viscosity ν. The mean energy dissipation rate $\varepsilon \equiv 2\nu\Omega$ where the enstrophy $\Omega \equiv \langle\omega^2\rangle$, and $\omega \equiv \boldsymbol{\nabla}\times\boldsymbol{u}$ is the vorticity. The Kolmogorov length is defined as $\eta \equiv (\nu^3/\varepsilon)^{1/4}$, the characteristic timescale of dissipation is given by $\tau_\eta = (\nu/\varepsilon)^{1/2}$, and $u_\eta \equiv \eta/\tau_\eta$ is the characteristic velocity scale at the dissipation length scale. In what follows, unless otherwise stated, we use η, τ_η, and u_η to nondimensionalize length, time, and velocity, respectively. The large-eddy turnover time is given by $T_{\mathrm{eddy}} \equiv 1/(k_f u_{\mathrm{rms}})$. We define the Stokes number as $\mathrm{St} \equiv \tau/\tau_\eta$, where τ is the particle response time in Eq. (1). As mentioned in the Introduction, this parameter measures the importance of particle inertia. Parameters of our simulation are given in Table I.

It is important to note that the particles in our simulations are actually point particles. As particle-particle interactions are ignored there are no real collisions. As far as the numerical code is concerned, the particles are characterized by the timescale τ which determines the Stokes number. To estimate the radius of a particle from its Stokes number we have used typical values of the ratio of the density of the particle to the density of the background fluid that corresponds to water droplets in clouds [34]. To obtain collision velocities that correspond to dust in protoplanetary disks one must use a

TABLE I. Parameters for our DNS runs with N^3 collocation points: ν is the kinematic viscosity, N_p is the number of particles, $\mathrm{Re} \equiv u_\mathrm{rms}/(\nu k_\mathrm{f})$ is based on the forcing wave number k_f, ε is the mean rate of energy dissipation, $\eta \equiv (\nu^3/\epsilon)^{1/4}$ and $\tau_\eta \equiv (\nu/\epsilon)^{1/4}$ are the Kolmogorov length and timescales, respectively, and $T_\mathrm{eddy} \equiv 1/(u_\mathrm{rms} k_\mathrm{f})$ is the large-eddy-turnover time. The Mach number $\mathrm{Ma} = u_\mathrm{rms}/c_\mathrm{s} \approx 0.1$. We quote dimensionless numbers.

N	N_p	Re	$1/(k_\mathrm{f}\eta)$	$T_\mathrm{eddy}/\tau_\eta$
512	10^7	89	14.28	2.21

different value of the density ratio. Also, since the sizes of the dust grains are smaller than the mean-free path of the gas [2,3,35], we must use a different expression for the particle response time. It is obtained by replacing the mean free path ℓ in $\nu = \ell c_\mathrm{s}$ by the particle size a. This yields $\tau \sim a$ instead of the quadratic dependence $\tau \sim a^2$ in Stokes law.

III. THEORETICAL BACKGROUND

In this section we summarize the dissipation-range theory for the distribution of relative velocities between two particles with different Stokes numbers [21]. We denote the relative-particle velocity by $\boldsymbol{V} = \boldsymbol{v}_2 - \boldsymbol{v}_1$, where $\boldsymbol{v}_1$ and $\boldsymbol{v}_2$ are the individual particle velocities. The distance between the particles is denoted by $R = |\boldsymbol{R}|$, where $\boldsymbol{R} = \boldsymbol{x}_2 - \boldsymbol{x}_1$ is the separation vector between the particle positions, and the longitudinal relative velocity is defined as $V_R = \boldsymbol{V} \cdot \boldsymbol{R}/R$. We denote the steady-state distribution of relative velocities and separations by $\mathscr{P}(R, V_R)$. The moments of the distribution are characterized by

$$\langle |V_R|^p \rangle \equiv \frac{m_p(R)}{m_0(R)}, \; m_p(R) = \int dV_R \, |V_R|^p \, \mathscr{P}(R, V_R). \tag{3}$$

The factor $m_0(R)$ is related to the pair correlation function $g(R)$ by $m_0(R) \propto g(R) R^{d-1}$ [6].

A. Distribution of relative velocities and separations

Gustavsson and Mehlig [6,14,15] developed a theory for the distribution of relative velocities of nearby *identical* particles. The theory takes into account particle inertia, and it rests on the observation that such particles form fractal spatial patterns in turbulence [26], and that caustics can give rise to large relative velocities at small separations [36–38]. The theory predicts that the distribution of relative velocities V_R at small separations R is a power law, reflecting fractal clustering in phase space. The power-law exponent is related to the phase-space correlation dimension D_2 [6,14,21]. The distribution determines the scaling of relative-velocity moments (3) with separation R [15]. These predictions for *identical* particles should hold for turbulence as well as statistical-model flows. In the white-noise limit, the theory was derived from first principles in Refs. [6,14]. For turbulent flows, the theoretical predictions were verified using DNSs [19,20,39] and using kinematic turbulence simulations [15]. See also Refs. [40–43].

The correlation dimension D_2 is not universal. In the white-noise limit D_2 can be calculated in perturbation theory [14,26], but in general it must be determined numerically. As is well known, D_2 depends nonmonotonically on St with a minimum at St of order unity [44].

Particles with *different* Stokes numbers cluster on distinct fractal attractors, so that the distribution of separations between particles with different Stokes numbers is cut off at a small spatial scale, R_c, that depends on the difference between the Stokes numbers [24,25]. How are the relative velocities of nearby particles affected? In Ref. [21] a statistical model for relative velocities between particles with different Stokes numbers was analyzed in the white-noise limit. It was shown that there is a distinctive velocity scale V_c, and that the distribution of V_R and R is a broad Gaussian below these scales [21], in other words approximately uniform:

$$\mathscr{P}(R, V_R) = \mathscr{N} R^{d-1} \begin{cases} 1 & \text{for } |V_R| < V_\mathrm{c} \text{ and } R < V_\mathrm{c}/z^*, \\ R^{\mu_\mathrm{c}-d-1} & \text{for } R > V_\mathrm{c}/z^* \text{ and } |V_R| < z^* R, \\ (|V_R|/z^*)^{\mu_\mathrm{c}-d-1} & \text{for } |V_R| > V_\mathrm{c} \text{ and } z^* R < |V_R|, \\ 0 & \text{for } |V_R| > V_0. \end{cases} \tag{4}$$

In addition to the normalization $\mathscr{N}$ there are four more parameters in Eq. (4): the two velocity scales V_c and V_0, the power-law exponent μ_c, and the parameter z^*.

The last parameter, z^*, defines the line $|V_R| = z^* R$ in the R-V_R plane where known limiting behaviors of $\mathscr{P}(R, V_R)$ in the dissipative range are matched to obtain the theoretical predictions for $\mathscr{P}(R, V_R)$.

The exponent μ_c is related to the phase-space correlation dimension $D_2(\overline{\mathrm{St}}\,)$ of the mono-disperse system with Stokes number $\overline{\mathrm{St}}$:

$$\mu_\mathrm{c} = \min\{D_2(\overline{\mathrm{St}}\,), d+1\}, \tag{5}$$

where $d = 3$ is the spatial dimension, and $\overline{\mathrm{St}}$ is the harmonic mean of the two Stokes numbers,

$$\overline{\mathrm{St}} = \frac{2\mathrm{St}_1 \mathrm{St}_2}{\mathrm{St}_1 + \mathrm{St}_2}. \tag{6}$$

The parameter D_2 can be calculated analytically in the white-noise limit [21,45,46], but in turbulent flows it must be determined numerically.

Now consider the upper velocity scale V_0. It was assumed in deriving Eq. (4) that it suffices to consider separations in the dissipative range where the turbulent fluid velocities are spatially smooth. This range extends up to separations R somewhat larger than the Kolmogorov length η. The theory

mirrors the distribution of spatial separations for $R < 1$ to distributions in relative velocities, just as it does for identical particles. Therefore the upper cutoff for the V_R power laws is

$$V_0 = z^*. \tag{7}$$

How this parameter depends upon the Stokes number is not known in general. In a one-dimensional statistical model this parameter was calculated in the white-noise limit in Ref. [6].

In Eq. (7), the distribution was simply set to zero for $V_R > V_0$. This is an oversimplification, in particular for turbulence where the far tails of the V_R distribution at small spatial separations result from particle pairs that have had separations in the inertial range in the past. For large Stokes numbers and when the inertial range is well developed it was argued in Ref. [12] that the tail of the conditional distribution $\mathscr{P}(R=0, V_R)$ has the form $\sim C_1/(\varepsilon\tau)^{1/2}\exp[-C_2|V_R|^{4/3}/(\varepsilon\tau)^{2/3}]$ for very large Stokes numbers. A statistical-model calculation with an inertial range yields the prefactors C_1 and C_2 in the white-noise limit, but they could have different parameter dependencies in turbulence [47]. At smaller Re, when the inertial range is not well developed, one may argue that the tail should be well approximated by a Gaussian with variance $\propto u_{\rm rms}^2$. The RMS turbulent velocity is an estimate of the relative velocities of particles that move independently at large separations of the order of the system size. In summary, the far tail of the relative-velocity distribution is not universal. Here we simply set

$$V_0 = u_{\rm rms} \tag{8}$$

when we compare with our DNS data.

The fourth parameter in Eq. (4) is the scale $V_{\rm c}$. It depends upon the difference of the two Stokes numbers. We follow Ref. [21] and write

$$\theta = \frac{|{\rm St}_1 - {\rm St}_2|}{{\rm St}_1 + {\rm St}_2}. \tag{9}$$

The white-noise model predicts that [21]

$$V_{\rm c} \propto \theta \tag{10}$$

at small θ. In this case, the power-law tails of the distribution (4) are expected to contribute to the relative velocity moments. According to Eq. (4), the tails of the distribution beyond $V_{\rm c}$ are simply those of the monodisperse system.

Equation (4) implies that the distribution of separations becomes uniform in R for $R < R_{\rm c}$, as predicted in Refs. [24,25]. Their spatial scale $R_{\rm c}$ is thus related to our velocity scale as follows:

$$R_{\rm c} \equiv V_{\rm c}/z^*, \tag{11}$$

and therefore $R_{\rm c} \propto \theta$ at small θ.

B. Moments of relative velocities

Theoretical predictions for $\langle|V_R|^p\rangle$ are obtained by integrating the distribution $\mathscr{P}$, as determined by Eq. (3). We first quote the results when θ is small, when the distribution exhibits a clear power law. This power law is cut off at small relative velocities at $\max(V_{\rm c}, z^*R) = z^*\max(R_{\rm c}, R)$, and consequently the result for $\langle|V_R|^p\rangle$ depends on whether $R > R_{\rm c}$ or not. When $R > R_{\rm c}$ we find

$$m_p(R) = b_p R^{\mu_{\rm c}+p-1} + c_p R^{d-1}, \tag{12}$$

with

$$b_p = -\frac{\mathscr{N}(1+d-\mu_{\rm c})z^{*p+1}}{(p+1)(\mu_{\rm c}-d+p)},$$
$$c_p = \frac{\mathscr{N}z^{*p+1}\left(\frac{V_0}{z^*}\right)^{\mu_{\rm c}-d+p}}{\mu_{\rm c}-d+p}, \tag{13}$$

where $\mathscr{N}$ is the normalization factor in Eq. (4). For large values of p, the coefficients b_p and c_p are sensitive to the form of the distribution beyond the cutoff z^*, which depends on the nature of the turbulent fluctuations. Also, the value of $\mu_{\rm c} = D_2(\overline{\rm St}\,)$ is not universal, and neither is the parameter z^*. The second term in Eq. (12) appears due to presence of singularities (of the gradient of particle velocity) called caustics [37,38] for nonzero values of St. In other words, the presence of caustics imply that while the distance between two nearby particles goes to zero their relative velocities can remain order unity. Whereas, in the absence of caustics, the particle velocity field remains smooth: relative velocity of two particles goes to zero as the separation between them goes to zero, and this gives rise to the first term in Eq. (12) (see Ref. [6] for more discussion).

The R dependence predicted by Eq. (12) is universal. It is equal to the scaling form of $m_p(R)$ for identical particles [15], as expected for small θ. But for particles with different Stokes numbers the coefficients b_p and c_p depend upon θ, although only through the global normalization constant $\mathscr{N}$. The scale $V_{\rm c}$ does not enter explicitly because $R > R_{\rm c}$.

Now consider $R < R_{\rm c}$. Then the uniform part in Eq. (4) dominates the moments. At $R < R_{\rm c}$, particles of two different sizes a_1 and a_2 move approximately independently from each other. In this case the moments take the form

$$m_p(R) \sim c_p' R^{d-1}, \tag{14}$$

with

$$c_p' = c_p - \frac{\mathscr{N}(1+d-\mu_{\rm c})(V_{\rm c}/z^*)^{\mu_{\rm c}-d+p}z^{*p+1}}{(\mu_{\rm c}-d+p)(p+1)}. \tag{15}$$

For $p = 1, 2, 3, \ldots$ one finds that $c_p' < c_p$ for heavy particles in incompressible turbulence at not too large Stokes numbers [DNSs show that $D_2 > d-1$, and that $D_2 < d+1$ for not too large Stokes numbers; see Eq. (5)]. The moments for larger θ are nevertheless usually larger than those for $\theta \to 0$, because the term $b_p R^{D_2+p-1}$ makes a large negative contribution unless R is extremely small, and this term is absent in Eq. (14). In general, if $\overline{\rm St}$ is small enough so that caustics are rare, then Eq. (14) can give a contribution for different particles that is much larger than for identical particles, leading to a significantly higher collision rate. The dependence on R is of the same form as the caustic contribution in Eq. (3) in the limit $\theta \to 0$.

Finally consider larger values of θ, large enough so that the power laws in Eq. (4) disappear. In a Gaussian white-noise model the distribution $\mathscr{P}(R, V_R)$ is Gaussian in this limit [21].

Very dissimilar pair of particles

When one of the particles has a very small Stokes number, e.g., $\mathrm{St}_2 \ll 1$, we can evaluate the coefficient c'_p term in Eq. (14) in terms of single-particle observables. We now outline the calculation for $p = 2$. When $\mathrm{St}_2 \ll 1$, we can expand the equation of motion up to leading order in St_2 to obtain the velocity of the second particle:

$$\boldsymbol{v}_2 \approx \boldsymbol{u}(\boldsymbol{x}, t) - \mathbb{A} \cdot \boldsymbol{R} - \mathrm{St}_2 \frac{D\boldsymbol{u}}{Dt}(\boldsymbol{x} + \boldsymbol{R}, t). \tag{16}$$

The relative velocity between two particles can then be written as

$$\boldsymbol{V}(\boldsymbol{R}) \approx \boldsymbol{v} - \boldsymbol{u}(\boldsymbol{x}, t) + \mathbb{A} \cdot \boldsymbol{R} + \mathrm{St}_2 \frac{D\boldsymbol{u}}{Dt}(\boldsymbol{x} + \boldsymbol{R}, t). \tag{17}$$

The first line of the right-hand side of Eq. (17) is St_1 times the acceleration of a *single* particle; at small $|\boldsymbol{R}|$ and St_2 this is the leading order contribution to the relative velocity. The distribution of the acceleration has been studied extensively and is known to have exponential tails [48,49]. This information allows us to approximately relate the structure functions to single-particle averages, as shown below.

We assume that to calculate $\langle V_R^2 \rangle$ for R much smaller than R_c it is sufficient to consider one component of $\boldsymbol{V}$. Consider one component of Eq. (17), square both sides of the resultant equation and then take steady-state averages. Assuming that $R \ll 1$ we obtain

$$\langle V_R^2 \rangle \approx \frac{1}{3}[\langle \boldsymbol{u}^2 \rangle - \langle \boldsymbol{v}^2 \rangle]\left(1 - 2\frac{\mathrm{St}_2}{\mathrm{St}_1}\right) - \frac{2}{3}\mathrm{St}_2 \langle (\boldsymbol{u} - \boldsymbol{v}) \cdot \mathbb{A} \cdot (\boldsymbol{u} - \boldsymbol{v}) \rangle. \tag{18}$$

All averages on the right-hand side of Eq. (18) are evaluated for a single particle with Stokes number St_1. The only St_2 dependence appears in the prefactors on the right-hand side of Eq. (18). We note that there is no R dependence (since all averages are single-particle averages). This is the result of neglecting the gradient term $\mathbb{A} \cdot \boldsymbol{R}$ in the equation for the particle separations. As explained in Sec. II A of Ref. [21] this is allowed provided that $R < R_c$. But note that in Ref. [21] the *white-noise model* was analyzed, while Eq. (18) applies to a turbulent flow.

IV. DNS RESULTS

A. Distribution of relative velocities and separations

Figure 1 shows a comparison between the theory Eq. (4) and our DNS results for $\mathscr{P}(R, V_R)/R^2$ for different values of θ. The first column of panels in this figure shows contour plots of $\mathscr{P}(R, V_R)/R^2$. As predicted by the theory (4), there is a region in the R-V_R plane where the distribution is a broad Gaussian. In a log-log plot this appears as an approximately uniform region where $\mathscr{P}/R^2$ is approximately constant. Outside this region, and for small values of θ, the equidistant contour lines show that the distribution exhibits the power laws, as predicted by the theory.

To analyze the power laws in relative velocities in more detail, the second column of panels in Fig. 1 shows plots of $\mathscr{P}(R, V_R)/R^2$ as functions of $|V_R|$ for several different values of R. We can clearly distinguish the power law from the broad Gaussian at small $|V_R|$, where $\mathscr{P}/R^2 \approx$ const. Equation (4) says that the crossover between these two behaviors occurs at $\min(V_c, z^* R)$. We estimate this crossover velocity scale by drawing two lines: a horizontal one at small $|V_R|$ and a power-law fit for larger $|V_R|$. The scale at which these two lines intersect is our estimate of the crossover scale. For small values of R the fits yield a velocity scale that is independent of R, this is V_c. For slightly larger values of R, the velocity scale is proportional to R, as predicted by theory, and the constant of proportionality defines the parameter z^*.

Dissipation-range theory [21] says that $V_c = c\,\theta$ for small θ, but the theory does not determine the constant of proportionality c. This constant is system specific, as is the value of z^*. In the white-noise limit these parameters can be calculated analytically [6,21], but not in general.

Therefore it is important to determine these constants by DNSs. The results are shown in Fig. 2. Figure 2(a) shows that z^* is essentially independent of θ, while Fig. 2(b) demonstrates that V_c is proportional to θ at small θ, as predicted by the theory. Figure 2(b) also shows that the prefactor depends on $\overline{\mathrm{St}}$ as $\overline{\mathrm{St}}^{1/2}$, at least for the parameters simulated. This follows from the fact that the DNS data for $V_c\,\overline{\mathrm{St}}^{-1/2}$ collapse onto a single line. However, there is no theoretical explanation for this result, as far as we know.

Figure 2(c) shows the power-law exponents μ_c. We extracted μ_c for different values of $\overline{\mathrm{St}}$ and for two different values of θ by fitting power laws to the DNS results for the distribution of relative velocities. Figure 2(c) shows the resulting exponents μ_c together with D_2 for the case $\mathrm{St}_1 = \mathrm{St}_2$ from Ref. [20]. Up to the numerical accuracy in our DNSs we find for $D_2 < 4$ that $\mu_c = D_2$, independent of θ for small values of θ. The phase-space correlation dimension D_2 has a characteristic minimum at $\overline{\mathrm{St}}$ of order unity and monotonously approaches the spatial dimension d for small $\overline{\mathrm{St}}$ and the dimensionality of phase space, $2d$, for large $\overline{\mathrm{St}}$ [see Fig. 2(c)].

In summary we observe good agreement between our DNSs and the theory, Eq. (4), in particular for small θ. As θ increases, the velocity scale V_c grows so that the range of the power law between V_c and V_0 becomes smaller. For large enough values of θ, the power laws disappear. In this limit the distribution is a broad Gaussian, approximately uniform. In our log-log plots, $\mathscr{P}/R^2$ is approximately constant in this region.

B. Moments of relative velocities

Figure 3 summarizes our DNS results for the moments of relative velocities as a function of particle separation. Figure 3(a) shows DNS results for $m_0(R)/R^2$ as a function of R (symbols), while Fig. 3(b) shows $m_2(R)/R^2$, also as a function of R. The parameters are given in the figure caption. Also shown is the scaling of the smooth contribution predicted by Eq. (12) (solid line). Dashed vertical lines correspond to the scale $R_c = V_c/z^*$. The parameters V_c, μ_c, and z^* were determined separately, as described in Sec. IV A.

As predicted by Eq. (12), the moments scales as R^{d-1} for $R < R_c$. For $R > R_c$ the smooth contribution dominates for

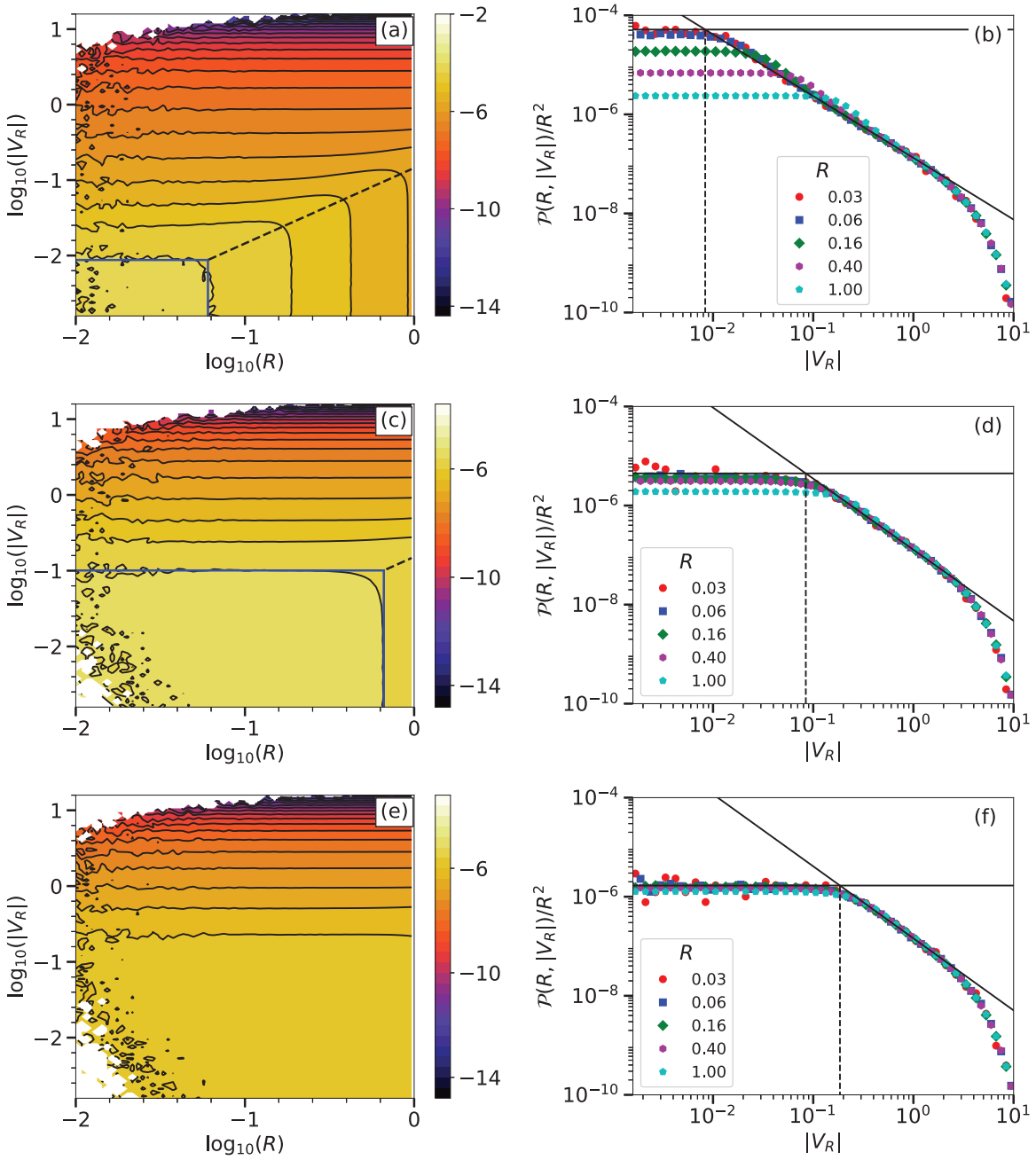

FIG. 1. DNS results for joint distribution $\mathscr{P}(R,|V_R|)$ of R and $|V_R|$, divided by R^2. Parameters: $\overline{\mathrm{St}}=2$ and $\theta=0.005$ (top row), $\theta=0.05$ (second row), and $\theta=0.1$ (bottom row). First column: Contour plots of $\mathscr{P}(R,|V_R|)/R^2$ color coded according to $\log_{10}[\mathscr{P}(R,|V_R|)/R^2]$. The blue lines in the bottom left corner of these plots show the scales R_c and V_c (see text). The dashed lines show the theoretical matching condition $|V_R|=z^*R$ (see text). Second column: plots of $\mathscr{P}(R,|V_R|)/R^2$ as functions of $|V_R|$ for different values of R as indicated in the panels. Also shown are fits (solid lines) to the theoretical power-law prediction $|V_R|^{\mu_c-4}$, Eq. (4), to determine μ_c as a function of $\overline{\mathrm{St}}$. The crossover between the approximately uniform (broad Gaussian) part at small $|V_R|$ (and small $R=0.03, 0.06$, horizontal solid lines) and the power law at intermediate R sets the scale V_c (dashed vertical lines).

$m_0(R)$ for both values of $\overline{\mathrm{St}}$, whereas for higher order moment $m_2(R)$ the smooth contribution dominates only for the smaller mean Stokes number. For larger mean Stokes number, the caustic contribution c_pR^{d-1} swamps the smooth part for R below R_c. In this limit the relative-velocity moments $m_p(R)$ are dominated by the singular R^{d-1} contribution provided that p is large enough. While the R dependence of this contribution is the same for identical particles and for particles with different Stokes numbers, the physical origin of this power law is slightly different in the two cases. For identical particles, the singular term is caused by caustics [36–38]. For particles with different Stokes numbers, by contrast, the singular contribution is due to the uncorrelated motion between nearby ($R<R_c$) particles with different Stokes numbers [21].

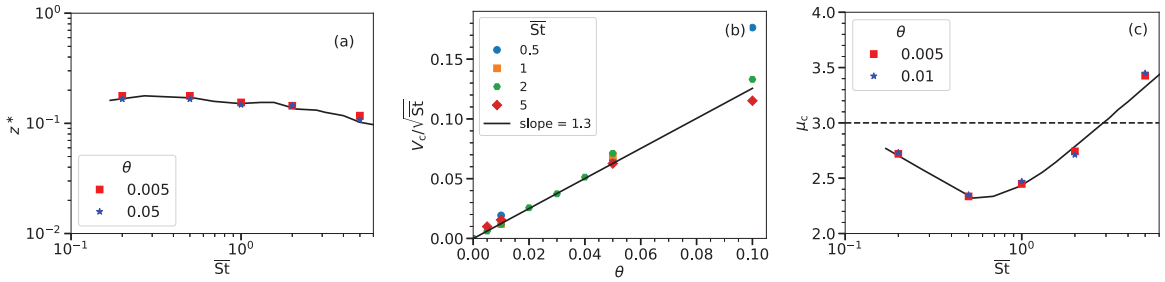

FIG. 2. Estimates of the parameters z^*, V_c, and μ_c, obtained from the DNS results for $\mathscr{P}(R, V_R)$ shown in Fig. 1. (a) Scale z^* as a function of $\overline{\mathrm{St}}$, for two different values of θ (symbols). The solid black line is the estimate for identical particles, taken from the DNSs of Ref. [20]. (b) Scale V_c as a function of θ (symbols), for different values of $\overline{\mathrm{St}}$. The solid black line shows a linear dependence upon θ with fitted prefactor 1.3. (c) Exponent μ_c as a function of $\overline{\mathrm{St}}$ for two different values of θ obtained by power-law fits to DNS results for $\mathscr{P}(R, V_R)$ at fixed R; see Fig. 1. The solid black line is the phase-space correlation dimension D_2 of the fractal attractor for identical particles with Stokes number $\overline{\mathrm{St}}$, taken from Ref. [20].

Very dissimilar pair of particles

Figure 3(c) shows DNS results for $\langle V_R^2 \rangle$ at the collision radius $R = a_1 + a_2$ for $\mathrm{St}_2 \ll 1$ as a function of St_1 (red circles), that is, for large values of θ. Also shown is the theoretical expression, Eq. (18) (green squares). The averages on the right-hand side of Eq. (18) are determined by DNSs, by averaging along heavy-particle paths in the steady state. The agreement is good at small values of St_1, but we observe deviations at larger values of the Stokes number. It is possible that this is due to higher-St_2 terms neglected in (18). Plotting only the first term of Eq. (18) yields slightly different results, although the deviations are smaller than those between the full theory and the DNS results.

We have checked that the gradient term $\mathbb{A} \cdot \boldsymbol{R}$ in the equation of motion for the separation $\boldsymbol{R}$ is negligible. For all data points shown, θ is large enough so that $a_1 + a_2$ is much less than R_c. In this range the DNS results do not depend upon R. This is the plateau region seen in Fig. 3(a).

V. DISCUSSION

Our results show in agreement with the theory that the distribution of relative velocities is non-Gaussian when θ is small. For a fairly wide range of θ (up to $\theta \sim 0.1$), the distribution has power-law tails $\sim |V_R|^{\mu_c - 4}$ at small separations. The dissipation-range theory predicts that the exponent μ_c is determined by the *phase-space* correlation dimension $D_2(\overline{\mathrm{St}})$ for a monodisperse system with Stokes number $\overline{\mathrm{St}}$ [Eq. (5)]. In our simulations, the numerical values of μ_c vary from approximately 2.4 to 3.5, and in this range there is good agreement between the theory and the numerical values of μ_c obtained from the DNSs [50].

In the astrophysical literature, several papers have reported DNS results for the distribution of relative particle velocities [13,17,18]. These authors attempted to fit the distributions to stretched exponentials, of the form $\exp[-(|V_R|/\beta)^\gamma]$ with fitting parameters β and γ. The parameter γ is usually quoted to be smaller than unity. This law is consistent neither with our power-law predictions nor with the large-St prediction from Ref. [12]. We have reanalyzed the data in Fig. 12 of Ref. [13] for the two smallest Stokes numbers, and find clear power laws over one decade of V_R/u_η, with exponents $\mu_c - 4$ in good agreement with the dissipation-range theory (the values of μ_c were obtained from the plots of the pair correlation function in Fig. 8 of the same paper).

We remark that the distribution of relative velocities in bidisperse suspensions was recently studied in Ref. [51]. This study did not report power laws for the distribution of relative velocities. As our results show, possible reasons for the absence of power laws are, first, that the distributions were calculated at quite large separations (of the order of the Kolmogorov length, $R \sim \eta$). Second, the values of θ were

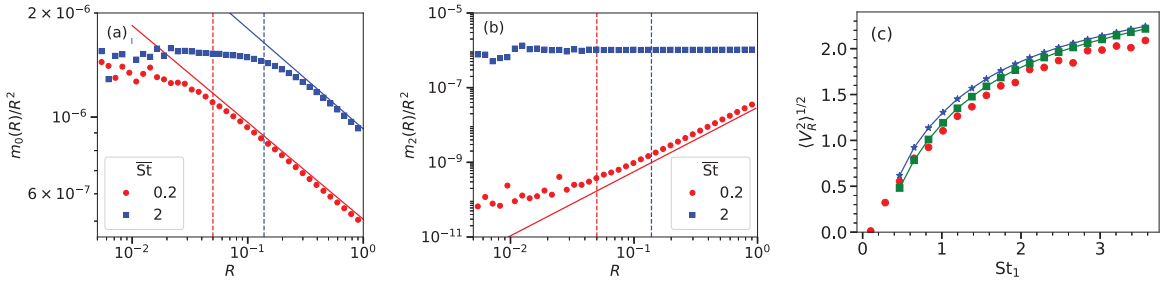

FIG. 3. DNS results for moments of relative velocities as a function of particle separation R. (a) Zeroth moment $m_0(R)$ and (b) second moment divided by R^2, for $\overline{\mathrm{St}} = 0.2$ and 2, and $\theta = 0.01$ (symbols). Solid line shows the scaling of smooth contribution in Eq. (12). The scale $R_c = V_c/z^*$ is indicated by the dashed vertical line. (c) Root-mean-square radial velocity $\langle V_R^2 \rangle^{1/2}$ for $R = a_1 + a_2$ plotted as a function of St_1 for $\mathrm{St}_2 = 0.1$ (red circles). The first term of theoretical estimate, Eq. (18), is plotted as blue ⋆ (joined with a blue solid line). The full expression Eq. (18), is plotted with green ■ (joined by a green solid line).

quite large, too large to see power laws as our theory and DNS data demonstrate.

Pan and Padoan [17] did not plot the radial relative velocity V_R (that determines how particles approach each other), but instead the RMS relative velocity $V_{\rm rms} \equiv \sqrt{V_1^2 + V_2^2 + V_3^2}$. The power law of the distribution of $V_{\rm rms}$ has a different exponent [6,14]: $|V_{\rm rms}|^{\mu_c - 2d}$. We have compared this prediction with the data shown in Fig. 14 of Ref. [17]. There is a clear power law, with exponent ≈ -3.7 for St $= 1.55$. Theory says that the exponent should equal $D_2 - 6$, but Ref. [17] does not give values for the fractal correlation dimension D_2. Estimating D_2 from our data at St $= 1.55$ (albeit at a different Reynolds number), we find $D_2 - 6 \approx -3.4$, in reasonable but not perfect agreement with the DNS results of Ref. [17].

Ishihara *et al.* state that their distribution approaches a Gaussian when θ is not small. This is consistent with theory [21], predicting a broad Gaussian for the body of the distribution. In our log-log plots, Fig. 1, the broad Gaussian appears as a region where $\mathscr{P}/R^2$ is approximately constant. When θ is large enough, this region extends out to V_0, approximately equal to the RMS turbulent velocity, $u_{\rm rms}$. The form of the far tails beyond V_0 is difficult to determine, because the tails describe rare events, and since there is no theoretical prediction apart from the law predicted in Ref. [12]. Yet this applies only at large Stokes numbers, and when there is a well-developed inertial range.

In both cases, when θ is small and when it is large, the RMS relative velocity is determined by the upper cutoff, V_0. We have simply set $V_0 = u_{\rm rms}$ here, but this is a simplification. In general, the upper cutoff V_0 must also depend on particle inertia (Stokes number). We have neglected this dependence here. Taking $V_0 = u_{\rm rms}$ implies that the moments of particle relative velocities depend on the Reynolds number Re when determined by the upper cutoff V_0, since $u_{\rm rms}/u_\eta \propto {\rm Re}^{1/4}$ [52]. With our present computational capabilities we cannot explore such a weak dependence on Re; hence we have concentrated our efforts on a single value of Re. Experimental data [23] confirm that the Re dependence is quite weak.

Ishihara *et al.* [13], on the other hand, computed RMS relative particle velocities for different values of Re (Fig. 3 in their paper), obtaining a fairly strong dependence on Re. A possible explanation of this result is that Ishihara *et al.* evaluated $\langle V_R^2 \rangle$ at fixed separation $r = 10^{-3}L$. Changing Re while keeping the system size L the same changes the Kolmogorov length η, and hence $R = r/\eta$ is different for different value of Re. Unless $R < R_c$ (whether this condition is satisfied or not is determined by the values of the Stokes numbers), the relative velocity statistics depends on R, as the dissipation-range theory shows. Thus evaluating the moments at $r = 10^{-3}L$ for changing η may give rise to a spurious Re dependence. It would be of interest to test quantitatively whether the Re dependence predicted by the dissipation-range theory is consistent with this explanation.

It is a strength of the dissipation-range theory summarized in Sec. III that it predicts how the moments of relative velocities depend upon particle separation R. The microscopic dust grains in accretion disks are much smaller than the Kolmogorov length η, so that the collision radius $R = a_1 + a_2$ is well below η. Inertial-range theories [8–12] do not refer to scales below η. As a consequence they cannot describe collisions that occur deep in the dissipation range. In DNSs it is also difficult to reach to such small scales, much smaller than η, simply because particles rarely come so close. But collisional aggregation in turbulent aerosols is fluctuation dominated when the systems are dilute, so that such rare events matter. Several recent works [13,17,53] give results for RMS relative velocities at fixed separations, usually of order η, irrespective of the size of the particles. The theory (12)–(15) allows us to extrapolate the DNS results to $R = a_1 + a_2$. Here the parameter $R_c = V_c/z^*$ plays an important role. If $R < R_c$, then the theory shows that the relative particle-velocity statistics is independent of the separation R.

A weakness of the dissipation-range theory is that it expresses the prefactors b_p and c_p in the R dependence of the moments in terms of parameters z^*, μ_c, V_c, and V_0 that must be determined separately, by DNSs, for example. The theory shows, moreover, that the prefactors are not universal. It would therefore be of great interest to find alternative ways of computing these prefactors. One possibility, although numerical, is to use the approach of Zaichik and collaborators [54,55] and its refinements [56].

VI. SUMMARY AND CONCLUSIONS

Let us summarize the key findings here. We used direct numerical simulations of particle-laden, homogeneous, and isotropic, forced turbulence to study the statistics of relative velocities and separations between particles with different Stokes numbers. We computed the joint distribution of particle separations and their relative velocities. We found that the shape of the distribution is in good agreement with the predictions of dissipation-range theory [21]. When the difference between the two Stokes numbers is small enough, then the distribution exhibits power laws, and the exponent is related to fractal patterns in phase space [26]. We found that the power laws are cut off at small relative velocities, at a scale V_c. We found that V_c depends linearly on θ for small values of θ, in agreement with the theoretical prediction [21].

When θ is large, by contrast, theory predicts that the body of the distribution is broad Gaussian [21], in agreement with the DNSs of Refs. [13,53]. In a log-log plot (Fig. 1) this Gaussian appears as a region where $\mathscr{P}/R^2$ is roughly constant. The shape of the distribution beyond V_0 (here simply set to zero) is not known. There are indications [53] that the theory of Ref. [12] may work for the tails. But this could not be unequivocally shown, and it must be borne in mind that the prediction of Ref. [12] applies to large Stokes numbers in systems with a very well developed inertial range, so that the scale-dependent Stokes number at the largest scale is much less than unity. These questions remain for further studies.

Dissipation-range theory [6,14–16,21] predicts how the relative-velocity fluctuations depend on particle separation. This power-law dependence of the relative-velocity moments upon particle separation is universal (but the prefactors of the power laws are not). The original inertial-range theories discussed above do not refer to particle separations in the dissipation range, and attempts to modify inertial-range theories to take into account dissipation-range dynamics [57,58] were

shown to fail (Fig. 5 in Ref. [13]), so that they cannot be used to model collision velocities of microscopic dust grains in circumstellar accretion disks, where collisions happen in the dissipation range. It is challenging to use DNSs to determine collision rates and velocities of small grains deep in the dissipation range, because such encounters are infrequent, yet significant. Usually, DNS data on relative-particle velocities [13,17,53] are evaluated at fixed separations of order η, as discussed above. The theory described and tested here allows one to extrapolate the DNS results to the relevant scales, often much smaller than the Kolmogorov length η.

Note added in proof. Note that Eq. (18) is essentially an expansion in powers of St_2 for small St_2, where we have retained terms up to first order in St_2. We have checked from our DNS that the correlation function on the second line of Eq. (18) is always negative and is proportional to ${\mathrm{St}_1}^2$ for small St_1. Eq. (18), which is confirmed by our DNS [Fig. 3(c)], is clearly in disagreement with Abrahamson's theory [59] which predicts that the RMS relative velocity of two inertial particles is given by the sum of their individual RMS velocities. This disagreement becomes apparent if we take the limit $\mathrm{St}_2 \to 0$ in Eq. (18), in which case the RMS relative velocity appears as the *difference* between the RMS velocities of an inertial particle and a tracer. It comes about because Ref. [59] assumes that the motions of the two particles are uncorrelated – an approximation of dubious validity when the particles are close to each other, i.e., about to collide. This again illustrates one of the central messages of this paper: a theory of relative velocity of two particles must take into account the distance between them, for otherwise the theory will fail to predict collision velocities.

ACKNOWLEDGMENTS

This work is supported by the grant Bottlenecks for Particle Growth in Turbulent Aerosols from the Knut and Alice Wallenberg Foundation (Dnr. KAW 2014.0048), by Vetenskapsradet (Grants No. 2013-3992 and 2017-03865], and by Formas (Grant No. 2014-585). The computations were performed on resources provided by the Swedish National Infrastructure for Computing (SNIC) at PDC. D.M. and A.B. thank John Wettlaufer for useful discussions.

[1] H. R. Pruppacher and J. D. Klett, *Microphysics of Clouds and Precipitation* (Springer Science & Business Media, Dordrecht, Netherlands, 2010), Vol. 18.

[2] M. Wilkinson, B. Mehlig, and V. Uski, Stokes trapping and planet formation, Astrophys. J. Suppl. **176**, 484 (2008).

[3] P. J. Armitage, *Astrophysics of Planet Formation* (Cambridge University Press, Cambridge, 2010).

[4] A. Johansen, J. Blum, H. Tanaka, C. Ormel, M. Bizzaro, and H. Rickman, in *Protostars & Planets VI*, edited by H. Beuther, R. S. Klessen, C. P. Dullemond, and T. Henning (University of Arizona Press, Tucson, 2014), p. 944.

[5] S. J. Weidenschilling and J. N. Cuzzi, Formation of planetesimals in the solar nebula, in *Protostars and Planets III* (University of Arizona Press, Tucson, 1993), p. 1031.

[6] K. Gustavsson and B. Mehlig, Relative velocities of inertial particles in turbulent aerosols, J. Turbulence **15**, 34 (2014).

[7] F. Windmark, T. Birnstiel, C. W. Ormel, and C. P. Dullemond, Breaking through: The effects of a velocity distribution on barriers to dust growth, Astron. Astrophys. **544**, L16 (2012).

[8] H. J. Völk, F. C. Jones, G. E. Morfill, and S. Roeser, Collisions between grains in a turbulent gas, Astron. Astrophys. **85**, 316 (1980).

[9] H. Mizuno, W. J. Markiewicz, and H. J. Völk, Grain growth in turbulent protoplanetary accretion disks, Astron. Astrophys. **195**, 183 (1988).

[10] W. J. Markiewicz, H. Mizuno, and H. J. Völk, Turbulence induced relative velocity between two grains, Astron. Astrophys. **242**, 286 (1991).

[11] B. Mehlig, V. Uski, and M. Wilkinson, Colliding particles in highly turbulent flows, Phys. Fluids **19**, 098107 (2007).

[12] K. Gustavsson, B. Mehlig, M. Wilkinson, and V. Uski, Variable-Range Projection Model for Turbulence-Driven Collisions, Phys. Rev. Lett. **101**, 174503 (2008).

[13] T. Ishihara, N. Kobayashi, K. Enohata, M. Umemura, and K. Shiraishi, Dust coagulation regulated by turbulent clustering in protoplanetary disks, Astrophys. J. **854**, 81 (2018).

[14] K. Gustavsson and B. Mehlig, Distribution of relative velocities in turbulent aerosols, Phys. Rev. E **84**, 045304 (2011).

[15] K. Gustavsson, E. Meneguz, M. Reeks, and B. Mehlig, Inertial-particle dynamics in turbulent flows: Caustics, concentration fluctuations, and random uncorrelated motion, New. J. Phys. **14**, 115017 (2012).

[16] K. Gustavsson and B. Mehlig, Statistical model for collisions and recollisions of inertial particles in mixing flows, Eur. Phys. J. E **39**, 55 (2016).

[17] L. Pan and P. Padoan, Turbulence-induced relative velocity of dust particles. I. Identical particles, Astrophys. J. **776**, 12 (2013).

[18] L. Pan, P. Padoan, and J. Scalo, Turbulence-induced relative velocity of dust particles. III. The probability distribution, Astrophys. J. **792**, 69 (2014).

[19] V. E. Perrin and H. J. J. Jonker, Relative velocity distribution of inertial particles in turbulence: A numerical study, Phys. Rev. E **92**, 043022 (2015).

[20] A. Bhatnagar, K. Gustavsson, and D. Mitra, Statistics of the relative velocity of particles in turbulent flows: Monodisperse particles, Phys. Rev. E **97**, 023105 (2018).

[21] J. Meibohm, L. Pistone, K. Gustavsson, and B. Mehlig, Relative velocities in bidisperse turbulent suspensions, Phys. Rev. E **96**, 061102 (2017).

[22] E.-W. Saw, G. P. Bewley, E. Bodenschatz, S. S. Ray, and J. Bec, Extreme fluctuations of the relative velocities between droplets in turbulent airflow, Phys. Fluids **26**, 111702 (2014).

[23] Z. Dou, A. D. Bragg, A. L. Hammond, Z. Liang, L. R. Collins, and H. Meng, Effects of Reynolds number and stokes number on particle-pair relative velocity in isotropic turbulence: A systematic experimental study, J. Fluid Mech. **839**, 271 (2018).

[24] J. Chun, D. L. Koch, S. L. Rani, A. Ahluwalia, and L. R. Collins, Clustering of aerosol particles in isotropic turbulence, J. Fluid Mech. **536**, 219 (2005).

[25] J. Bec, A. Celani, M. Cencini, and S. Musacchio, Clustering and collisions in random flows, Phys. Fluids **17**, 073301 (2005).
[26] K. Gustavsson and B. Mehlig, Statistical models for spatial patterns of heavy particles in turbulence, Adv. Phys. **65**, 1 (2016).
[27] A. Brandenburg and W. Dobler, Hydromagnetic turbulence in computer simulations, Computer Phys. Commun. **147**, 471 (2002).
[28] J. H. Williamson, Low-storage Runge-Kutta schemes, J. Comput. Phys. **35**, 48 (1980).
[29] A. Brandenburg, The inverse cascade and nonlinear alpha-effect in simulations of isotropic helical hydromagnetic turbulence, Astrophys. J. **550**, 824 (2001).
[30] D. J. Higham, An algorithmic introduction to numerical simulations of stochastic differential equations, SIAM Rev. **43**, 525 (2001).
[31] W. Dobler, N. E. L. Haugen, T. A. Yousef, and A. Brandenburg, Bottleneck effect in three-dimensional turbulence simulations, Phys. Rev. E **68**, 026304 (2003).
[32] N. E. L. Haugen, A. Brandenburg, and W. Dobler, Is nonhelical hydromagnetic turbulence peaked at small scales?Astrophys. J. Lett. **597**, L141 (2003).
[33] N. E. L. Haugen and A. Brandenburg, Inertial range scaling in numerical turbulence with hyperviscosity, Phys. Rev. E **70**, 026405 (2004).
[34] R. A. Shaw, Particle-turbulence interactions in atmospheric clouds, Annu. Rev. Fluid Mech. **35**, 183 (2003).
[35] P. S. Epstein, On the resistance experienced by spheres moving through gases, Phys. Rev. **23**, 710 (1924).
[36] G. Falkovich, A. Fouxon, and M. G. Stepanov, Acceleration of rain initiation by cloud turbulence, Nature (London) **419**, 151 (2002).
[37] M. Wilkinson and B. Mehlig, Caustics in turbulent aerosols, Europhys. Lett. **71**, 186 (2005).
[38] M. Wilkinson, B. Mehlig, and V. Bezuglyy, Caustic Activation of Rain Showers, Phys. Rev. Lett. **97**, 048501 (2006).
[39] M. V. Kuhle, A. Pumir, E. Lévêque, and M. Wilkinson, Prevalence of the sling effect for enhancing collision rates in turbulent suspensions, J. Fluid Mech. **749**, 841 (2014).
[40] J. Bec, L. Biferale, M. Cencini, A. Lanotte, and F. Toschi, Intermittency in the velocity distribution of heavy particles in turbulence, J. Fluid Mech. **646**, 527 (2010).
[41] J. Bec, L. Biferale, M. Cencini, A. Lanotte, and F. Toschi, Spatial and velocity statistics of inertial particles in turbulent flows, J. Phys.: Conf. Ser. **333**, 012003 (2011).
[42] J. P. L. C. Salazar and L. R. Collins, Inertial particle relative velocity statistics in homogeneous isotropic turbulence, JFM **696**, 45 (2012).
[43] M. James and S. S. Ray, Enhanced droplet collision rates and impact velocities in turbulent flows: The effect of polydispersity and transient phases, Sci. Rep. **7**, 12231 (2017).
[44] J. Bec, L. Biferale, M. Cencini, A Lanotte, S. Musacchio, and F. Toschi, Heavy Particle Concentration in Turbulence at Dissipative and Inertial Scales, Phys. Rev. Lett. **98**, 084502 (2007).
[45] M. Wilkinson, B. Mehlig, and K. Gustavsson, Correlation dimension of inertial particles in random flows, Europhys. Lett. **89**, 50002 (2010).
[46] K. Gustavsson, B. Mehlig, and M. Wilkinson, Analysis of the correlation dimension of inertial particles, Phys. Fluids **27**, 073305 (2015).
[47] K. Gustavsson and B. Mehlig, Distribution of velocity gradients and rate of caustic formation in turbulent aerosols at finite Kubo numbers, Phys. Rev. E **87**, 023016 (2013).
[48] J. Bec, L. Biferale, G. Boffetta, A. Celani, M. Cencini, A. Lanotte, S Musacchio, and F. Toschi, Acceleration statistics of heavy particles in turbulence, J. Fluid Mech. **550**, 349 (2006).
[49] A. Bhatnagar, Direct numerical simulations of fluid turbulence: (A) Statistical properties of tracer and inertial particles (B) Cauchy-Lagrange studies of the three-dimensional Euler equation, Ph.D. thesis, Dept. of Physics, Indian Institute of Science, Bangalore, 2016.
[50] This agreement should be understood in the following manner. The theory does not allow a calculation of μ_c from first principle, but it shows that $\mu_c = D_2(\overline{\mathrm{St}})$ for small θ. This is indeed what we confirm from DNSs .
[51] R. Dhariwal and A. D. Bragg, Small-scale dynamics of settling, bidisperse particles in turbulence, J. Fluid Mech. **839**, 594 (2018).
[52] This can be derived using the Kolmogorov scaling $u_{\mathrm{rms}}/u_\eta \sim (l_f/\eta)^{1/3}$, where $l_f = 1/k_f$ is forcing scale.
[53] L. Pan, P. Padoan, and J. Scalo, Turbulence-induced relative velocity of dust particles. II. The bidisperse case, Astrophys. J. Lett. **791**, 48 (2014).
[54] L. I. Zaichik, O. Simonin, and V. M Alipchenkov, Two statistical models for predicting collision rates of inertial particles in homogeneous isotropic turbulence, Phys. Fluids **15**, 2995 (2003).
[55] L. I. Zaichik, V. M. Alipchenkov, and E. G. Sinaiski, *Particles in Turbulent Flows* (John Wiley & Sons, 2008).
[56] L. Pan and P. Padoan, Relative velocity of inertial particles in turbulent flows, J. Fluid Mech. **661**, 73 (2010).
[57] C. W. Ormel and J. N. Cuzzi, Closed-form expressions for particle relative velocities induced by turbulence, Astron. Astrophys. **466**, 413 (2007).
[58] L. Pan and P. Padoan, Turbulence-induced relative velocity of dust particles V. Testing previous models, Astrophys. J. **812**, 10 (2015).
[59] J. Abrahamson, Collision rates of small particles in a vigorously turbulent fluid, Chem. Eng. Sci. **30**, 1371 (1975).